Atmos. Chem. Phys. Discuss., 4, 71–108, 2004
www.atmos-chem-phys.org/acpd/4/71/
SRef-ID: 1680-7375/acpd/2004-4-71


Atmospheric Chemistry and Physics Discussions

# Sources and distribution of trace species in Alpine precipitation inferred from two 60-year ice core paleorecords

**A. Eichler**[1, 2], **M. Schwikowski**[1], **M. Furger**[1], **U. Schotterer**[2], **and H. W. Gäggeler**[1, 2]

[1]Paul Scherrer Institute, CH-5232 Villigen PSI, Switzerland
[2]Department of Chemistry and Biochemistry, University of Bern, Freiestrasse 3, CH-3012 Bern, Switzerland

Received: 27 November 2003 – Accepted: 18 December 2003 – Published: 7 January 2004

Correspondence to: M. Schwikowski (margit.schwikowski@psi.ch)

## Abstract

The Alps represent the largest barrier to meridional air flow in Europe, strongly influencing the weather and hence the distribution of atmospheric trace components. Here for the first time, chemical records from two ice cores retrieved from glaciers located in the northern and southern Swiss Alps were compared in conjunction with an analysis of "weather type," in order to assess geographical and seasonal trends in the deposition of trace species and to identify source regions and transport patterns.

Using a correlation analysis, investigated trace species ($NH_4^+$, $NO_3^-$, $SO_4^{2-}$, $Ca^{2+}$, $Mg^{2+}$, $Na^+$, $K^+$, and $Cl^-$) were grouped into classes of different origin (anthropogenic, sea salt, or Saharan dust). Over the last 60 years, precipitation chemistry at both sites was dominated by $NH_4^+$, $NO_3^-$, and $SO_4^{2-}$, all of anthropogenic origin and deposited mainly in summer by way of convective precipitation. The similarity of the $SO_4^{2-}$ profiles with historical records of $SO_2$ emissions from France and Italy indicated these two countries as key source areas for the anthropogenic species.

In contrast, sea salt and Saharan dust showed major differences in transport pattern and deposition across the Alps. Currently, the sea-salt constituents $Na^+$, $K^+$, and $Cl^-$ are transported to the northern site during advective westerly-wind situations, independent of Saharan dust events. At the southern site, sea salt and Saharan dust are deposited simultaneously, indicating a coupled transport active mainly in summer during south-westerly wind situations.

## 1. Introduction

The European Alps extend over 1000 km from the Mediterranean Sea northward into Switzerland and then eastward into Austria. Their extent is larger than the typical synoptic scale and therefore the region is usually not subject to uniform weather. The Alps act as a barrier to air flow, thereby influencing strongly the central European climate. Typically, northern regions are more influenced by polar-maritime air masses,



ACPD

4, 71–108, 2004

whereas on the southern side, tropical-maritime air masses dominate. Moreover, the main Alpine chain effectively acts as a divide and induces north-south gradients in the distribution of atmospheric pollutants in Europe.

Snowpacks and glaciers in the Alps are well-suited natural archives of precipitation chemistry and atmospheric fluxes. The ice core records from cold alpine glaciers provide important information on past environmental conditions in Europe. To date, ice cores from three different high-alpine glacier sites have been used to reconstruct the air pollution history of central Europe: Fiescherhorngletscher (Bernese Alps, northern Alpine region), Grenzgletscher, Colle Gnifetti (Monte Rosa massif, southern Alps), and Col du Dôme (Mont Blanc massif, western Alps) (for review see Schwikowski, 2003). The temporal evolution of a number of chemical trace species and gases over the last 50-250 years has previously been investigated in several studies (Döscher et al., 1995; Döscher et al., 1996; Eichler et al., 2000b; Lavanchy et al., 1999; Legrand et al., 2002; Preunkert et al., 2001a; Preunkert et al., 2001b; Schwikowski et al., 1999a; Schwikowski et al., 1999b; van de Velde, 1999; van de Velde, 2000; Wagenbach et al., 1988). However, although comprehensive data sets for each of these high-altitude glacier sites in the Alps exist independently, comparative studies between different locations to investigate geographical variability in precipitation chemistry are rare.

Preunkert et al. (2000) compared concentration records of the main trace species between the Col du Dôme site and the Colle Gnifetti site (80 km to the east) in the period 1982–1991. Their results suggest, at least for the anthropogenic species $NH_4^+$, $NO_3^-$, and $SO_4^{2-}$, that the two Alpine sites likely experience similar atmospheric conditions throughout the entire year. However, difficulties arose in this comparative study, because a variable amount of the annual snow deposition (mainly winter snow) at the Colle Gnifetti site is removed by wind erosion. Another study on the geographical and seasonal distribution of atmospheric constituents at high elevation sites (above 3000 m a.s.l.) in the Alps was the SNOSP (SNOw Sampling Program) (see e.g. Nickus et al., 1997; Schwikowski et al., 1997). Within this program, snow concentrations and deposition fluxes of nine major ions ($NH_4^+$, $NO_3^-$, $SO_4^{2-}$, $Ca^{2+}$, $Mg^{2+}$, $Na^+$, $K^+$, $Cl^-$,

$H^+$) were determined at glaciers from the southwestern end of the French Alps to the eastern part of the Austrian Alps. For the period 1991–1993, this study documented a west-east gradient of ion concentration for high alpine snow, with higher values in the east (Nickus et al., 1997). However, the total fluxes were rather uniform because the gradients in concentration were compensated for by an opposite gradient in precipitation amount. A second study in the course of the SNOSP program was carried out in 1993–1994 at six sampling sites along a 120 km north-south transect in the eastern Alps (Nickus et al., 1998). Sulphate concentrations and sulphate-to-nitrate ratios in the southern part were found to be higher as compared to the north, which was related to a higher incidence of southerly airflow. Furthermore, a south-to-north decrease in $Ca^{2+}$, $Mg^{2+}$, and $K^+$ concentrations was detected and attributed to a decreasing influence of Saharan dust along the transect. However, it remains difficult to deduce general conclusions from the results of the SNOSP program, given that only winter and spring snow samples taken over just 2–3 years were considered, and the concentrations of certain ions are known to show pronounced seasonality.

Further investigations were carried out by Weiss et al. (1999), revealing that the Alps are an efficient barrier for the transport of atmospheric pollutants. They investigated the atmospheric Pb deposition in Switzerland on the basis of five rural peat bogs, covering the period between c. 1850 and 1990. A similar temporal pattern of Pb enrichment was found in four cores from western and central Switzerland, whereas the one study site in southern Switzerland revealed a completely different history with respect to Pb pollution. This study implied that the northern and southern Alpine sites are influenced by different pollution sources and atmospheric pathways. Comparable results were obtained from a study of the annual pollen influx at the forest limit in the Swiss Alps (van der Knaap et al., 2001). Four study sites along a north-south transect in the Swiss Alps were investigated during a seven-year period. The influx of extra-regional pollen derived from south of the Alps was found to be highest at the stations south of the Alps and lowest at the stations lying north of the central Alps, indicating the barrier effect of the Alps for southern air masses.



ACPD
4, 71–108, 2004

Here, we test the hypotheses of a north-to-south gradient in the deposition of the main ionic trace species ($NH_4^+$, $NO_3^-$, $SO_4^{2-}$, $Ca^{2+}$, $Mg^{2+}$, $Na^+$, $K^+$, $Cl^-$). Chemical data from two ice cores, retrieved from glaciers in the northern and southern Swiss Alps, were compared in order to assess geographical and seasonal trends in the distribution of atmospheric pollutants in Western Europe during the last ~60 years. We investigated also the patterns of weather conditions leading to precipitation at the two sites. Furthermore, statistical values (e.g. medians, correlations), annual cycles, and long-term trends in concentrations of the main trace species were investigated to determine differences in the source areas and transport pattern of these species in regards to both sites.

## 2. Site description

### 2.1. Drilling sites

#### 2.1.1. Fiescherhorngletscher (FG)

The study site within the northern Alpine chain is situated upon Fiescherhorngletscher (FG, Bernese Alps) (see Fig. 1). An ice core of 77-m length was recovered in 1989 at an elevation of 3890 m a.s.l. (46°32'53" N, 8°02'46" E) (Schwikowski et al., 1999a; Schotterer et al., 1997). The drilling site is located within a 0.5 $km^2$ plateau between the mountains Grossfiescherhorn (4049 m a.s.l.), Hinterfiescherhorn (4025 m a.s.l.), and Ochs (3900 m a.s.l.). Radar soundings performed in 2000 revealed a glacier thickness at the drilling site of about 150 m (M. Funk, personal communication, 2000). Based on a borehole temperature of −5.2°C at 7.5 m depth (J. Schweizer, personal communication, 1986), it was assumed that this part of the glacier lies within the recrystallisation-infiltration zone. Thus, the meltwater that forms occasionally at the surface is assumed to refreeze only a few centimetres below.

### 2.1.2. Grenzgletscher (GG)

The study site in the southern Alpine chain is situated within the upper reaches of the Grenzgletscher (GG, Valais Alps) near the Swiss-Italian border (see Fig. 1). The upper Grenzgletscher is embedded between the Monte Rosa summit Dufourspitze (4634 m a.s.l.) and the Liskamm (4527 m a.s.l.). A 125-m ice core was recovered in October 1994 at an elevation of 4200 m a.s.l. (45°55'28" N, 7°52'3" E) (Gäggeler et al., 1997). The glacier thickness at the drilling site is about 190 m (see e.g. Eichler et al., 2000a). Borehole temperatures showed that this portion of the upper Grenzgletscher belongs to the cold infiltration zone, where meltwater may be present in the upper firn layers (Suter et al., 2001).

## 2.2. Chemical analysis and dating of the ice cores

Both ice cores (of 7.8 cm diameter) were extracted with a custom-made electromechanical ice drill and cut into 0.5–0.8 m long sections at the drilling site. Subsequently, the individual core sections were packed and sealed in polyethylene sleeves and after subzero transport were kept frozen in a cold room at –20°C. The ice core sections were cut with a band saw into segments 5–20 cm long, in the process taking off the outermost 0.5–1.5 cm that could have possibly become contaminated. The decontaminated samples were allowed to melt in pre-cleaned plastic vials just prior to analysis. The determination of the main soluble inorganic cations ($Na^+$, $NH_4^+$, $K^+$, $Mg^{2+}$, $Ca^{2+}$) and anions ($F^-$, $Cl^-$, $NO_3^-$, $SO_4^{2-}$) was performed by ion chromatography with conductivity detection. For details regarding the sample preparation and the chemical analyses, see Eichler et al. (2000a) and Schwikowski et al. (1999a).

Dating of the FG ice core was performed by annual layer counting, using the seasonally-varying signals in both the oxygen-isotopic ratio ($\delta^{18}O$) and tritium activity concentration (Schwikowski et al., 1999a; Schotterer et al., 1997). Furthermore, characteristic reference horizons (a Saharan dust fall in 1977 and the maximum in atomic bomb testing in 1962) were used to corroborate the annual layer counting, re-



ACPD
4, 71–108, 2004

vealing that the 77 m (57 m water equivalent (w.eq.)) long ice core covers the time period 1944–1988. From this age scale, a mean annual accumulation rate of 1.4 m w.eq. was determined.

Dating of the GG ice core was performed via measurements of the naturally-occurring radioisotope $^{210}$Pb and by annual layer counting, utilising the strong seasonal pattern in both $NH_4^+$ concentrations and $\delta^{18}O$ values (Eichler et al., 2000a). Additionally, reference horizons were again used for dating confirmation (Saharan dust falls in 1947, 1977, and 1990, the maxima of the atmospheric nuclear weapon tests in 1962 and 1958, and the reactor accident in Chernobyl in 1986). The time period covered by the 125 m (104 m w.eq.) long ice core is 1937–1994 and the mean annual accumulation rate 2.7 m w.eq. (Eichler et al., 2000a). Due to an occurrence of meltwater percolation at the drilling site, chemical records in the section from 11 to 24 m w.eq. (corresponding to the years 1985–1989) were partly destroyed (Eichler et al., 2001). Especially influenced were the trace species $K^+$, $Na^+$, $Mg^{2+}$, $Ca^{2+}$, and $SO_4^{2-}$. In contrast, the primary seasonality seen within the concentrations of $NH_4^+$, $F^-$, $Cl^-$, and $NO_3^-$ was preserved. In the following discussions, the time period 1985–1989 was therefore excluded.

### 2.3. Precipitation characteristics at the ice core sites

In Switzerland, the areas receiving maximum precipitation (up to 4 m year$^{-1}$) occur across both the northern and southern Alps, because either Alpine chain can act as barrier to advecting air masses. The most frequent precipitation type in the northern Alps is that from polar-maritime air masses during westerly wind situations, whereas the southern Alps mainly experience precipitation from tropical-maritime air masses during föhn situations (see e.g. Bär, 1983).

To more precisely characterise those weather situations leading to precipitation at the two ice core sites, an analysis of "weather type" was performed. For this, the Alpine weather-type classification of M. Schüepp was used (for details see Fliri, 1984). In this classification, key parameters (e.g. surface and 500 hPa air stream, weather character

– cyclonic, anticyclonic and undifferentiated) are combined to define 32 Alpine weather situations. Fliri (1984) divided these 32 situations into 10 groups:

– eight advective groups (**NE, E, SE, S, SW, W, NW, N**), where the horizontal motion of the atmosphere is dominant and

– two convective groups: **L** (cyclonic + undifferentiated situations) and **H** (anticyclonic situations), where the weather is predominantly influenced by vertical motion.

Fliri (1984) quantified the relevance of each group for precipitation in Switzerland (period 1946–1979). These maps were used to determine the weather types leading to the most frequent precipitation in the northern and southern Alps in the areas of both drilling sites (see Table 1). In spring and autumn the situation is different at both sites; in the northern Alps precipitation occurs mainly during advective westerly-wind situations (W), whereas in the southern Alps precipitation during föhn situations (SW) is predominant. Additionally, convective precipitation during low pressure situations (L) occurs at both sites. In winter, precipitation is most frequently observed at both sites during advective westerly-wind situations (W). Precipitation resulting from moisture advected from the Northwest (NW) to the northern site and from the Southwest (SW) to the southern part is also important. In summer, both sites are mainly influenced by small-scale convective precipitation (L) leading to shower and thunderstorm activity and a predominant uniformity of Alpine weather. Additionally, advective precipitation from the West (W) affects both places during summertime.

This classification has been corroborated by correlation analyses of daily precipitation amounts between stations in the northern and southern Alps (Fliri, 1974). The lowest correlation coefficients were observed in spring and autumn, due to the different advective precipitation systems affecting the sites. A much higher degree of correlation was found in winter, whereas the highest correlation coefficients were obtained for the summer months.

The expected seasonal distributions of precipitation corresponding to the northern and southern ice core sites, on the basis of weather station data from Interlaken and Mosogno, respectively, are shown in Fig. 2. In the northern Alps, the precipitation

maximum is in summer and the minimum in winter. The warmer air masses in summer have the ability to take up more moisture over the ocean than the colder air masses in winter. Precipitation in the southern Alpine chain exhibits two maxima (in spring and autumn) due to precipitation during föhn situations, which are prevalent in both of these seasons.

Given the contrasting precipitation regimes affecting the two ice core sites, one would expect large differences in the deposition of trace species. Thus, the precipitation chemistry at the northern site should be more influenced by pollutants coming from the West, whereas pollutants deposited at the southern site should have come from the Southwest and West.

## 3. Results and discussion

### 3.1. Sources of trace species in precipitation

For comparing the respective concentration records of the main ionic species ($NH_4^+$, $NO_3^-$, $SO_4^{2-}$, $Ca^{2+}$, $Mg^{2+}$, $Na^+$, $K^+$, $Cl^-$) from the two ice cores, only the data from the period of overlap (1945–1983) were used. Within this 38-year period, the chemistry records were represented by 744 and 1386 samples for FG and GG, respectively. Hence, in order to achieve a similar time resolution for both ice cores, average values of consecutive pairs of samples were used throughout the GG record (resulting in 693 data values).

Median concentrations of the trace ions at both glacier sites reveal that the chemical composition of both ice cores (during 1945–1983) is dominated by the ions $NH_4^+$, $NO_3^-$, $SO_4^{2-}$, and $Ca^{2+}$, contributing about 80% to the overall ion budget on a molar basis (see Table 2). Thus, precipitation chemistry at both sites is determined mainly by trace species of anthropogenic origin (see below). This result is in accordance with the proximity of Alpine glaciers to the densely-populated and industrialised areas of Western Europe. Interestingly, the median concentrations themselves of these four ions ($NH_4^+$,

$NO_3^-$, $SO_4^{2-}$, and $Ca^{2+}$) and $Mg^{2+}$ are also similar at the two ice core sites (see Table 2). This result was not expected, because of the commonly dissimilar precipitation regimes (see Sect. 2.3). Only the concentrations of the less-abundant ions ($Na^+$, $Cl^-$, and $K^+$) differ significantly, as they are twice as high at the northern site (Table 2).

Correlation analyses performed on the concentration data (taken as the logarithm) were used to identify the main sources for the trace species (see Table 3). Here, a general assumption has been made that species showing high cross-correlation either have the same source, or if having different sources were nevertheless transported with the same air masses to the particular site. At both sites, concentrations of $NH_4^+$, $NO_3^-$, and $SO_4^{2-}$ are highly intercorrelated. Gaseous precursor species of these trace components (i.e. $NH_3$, $NO_x$, and $SO_2$) are emitted into the atmosphere primarily by anthropogenic means, specifically from agriculture, motorised vehicles, and combustion of fossil fuels, respectively (see e.g. Finlayson-Pitts and Pitts, 2000). Chemical reactions in the atmosphere lead to the formation of secondary aerosol components (e.g. $NH_4NO_3$, $NH_4HSO_4$, and $(NH_4)_2SO_4$), explaining the high correlation between the concentrations of these anthropogenically-derived species. However, it is surprising that the $K^+$ concentrations at GG are also highly correlated with the concentrations of $NH_4^+$, $NO_3^-$, and $SO_4^{2-}$, indicating that $K^+$ is partly of anthropogenic origin as well. This correlation is the first such observation in Alpine ice core studies. Measurements of the size-segregated aerosol composition at the high Alpine station Jungfraujoch (3580 m a.s.l.; Streit et al., 2000) showed a maximum in $K^+$ concentration in the small-particle range (accumulation mode: 0.1–1 $\mu$m diameter), likewise indicating anthropogenic sources such as emissions from coal or wood combustion (see e.g. Finlayson-Pitts and Pitts, 2000).

Soluble ion sources of mainly natural origin for the northern Alpine site are sea salt ($Na^+$, $Cl^-$, and $K^+$) and mineral dust ($Ca^{2+}$, $Mg^{2+}$) (see Schwikowski et al., 1999a). Despite having independent sources, concentrations of sea salt and dust-related species are well correlated for the GG. Studies of Wagenbach and Geis (1989) revealed that about two-thirds of the deposited dust in the southern Alps originates from the Saharan

desert. Our results from GG suggest furthermore that the transport of Saharan dust to the southern Alpine chain is coupled to the transport of sea salt (see Eichler et al., 2000b). In this case, the aerosol of sea salt composition has a source either directly in the Sahara, or is injected into trans-Saharan air masses during transport over the sea.

### 3.2. Annual cycle in concentrations of trace species

Both the mean composition and the correlation analyses at the two sites revealed only general sources for the major and minor ions in the ice cores. The determination of transport paths and source areas of these species, however, requires more detailed analyses. To begin, we compared the ice core records on a seasonal basis.

Only those samples from the 10-year period 1974–1983 were used in the comparison of the seasonally-resolved concentration records of trace species. This period was selected, given that the dating uncertainty of both records is less than one year only for this time period. Based on the seasonal evolution in the temperature-dependent parameter $\delta^{18}$O, the sample data were classified into winter, spring, summer, and autumn values (Eichler, 2000c). Schotterer et al. (1997) and Eichler et al. (2001) have shown that the ice core-$\delta^{18}$O values and the monthly averaged air temperatures at the nearby stations Jungfraujoch and Col du Gd. St. Bernard are well correlated for the FG (period 1983-84) and GG sites (period 1980–1994), respectively. The lowest temperatures as averaged over the period 1974–1983 were observed in January. Hence, after attributing samples with the lowest $\delta^{18}$O values to January, the annual layers were then divided into 12 sublayers of equal thickness. Subsequently, quarterly (three-month) periods were related to the commonly-defined seasons (e.g. the December-February period representing winter), and for each season the concentration average in the selected 10-year period was calculated. The seasonal cycles of the trace ion concentrations and $\delta^{18}$O values are shown in Fig. 3. The good correlation between the annual cycle of $\delta^{18}$O at the two locations and also with the air temperatures at Col du Gd. St. Bernard (2480 m a.s.l., Fig. 3), indicates that the four quarters



ACPD
4, 71–108, 2004

as defined indeed represent the actual seasons.

### 3.2.1. Trace species of anthropogenic origin

Concentrations of species with anthropogenic origin ($NH_4^+$, $NO_3^-$, $SO_4^{2-}$) at both sites show a similar seasonal cycle, with summer concentrations two- to three-times higher than in winter (Fig. 3, $NO_3^-$ not shown) (see also Table 4). Due to an enhanced convection regime in summer, aerosol-rich air from the atmospheric boundary layer reaches altitudes above 4000 m a.s.l. in the Alps (Lugauer et al., 1998). Thus, comparable convective precipitation occurs at the FG and GG sites (see Sect. 2.3.), which explains the high similarity in concentrations of those species with anthropogenic origin in summer. In winter, however, both sites lie within the free troposphere, due to the suppression of vertical motion by the stable stratification of the atmosphere. For this reason, advective precipitation in winter dominates and leads to the comparably low concentrations of trace species that represent specifically the conditions of the free troposphere. The relatively high summer:winter ratio of the $NH_4^+$ concentrations as compared to the analogous $NO_3^-$ and $SO_4^{2-}$ ratios (Table 4) is due to the different emission characteristics of the respective precursor species. While $NH_3$ is emitted predominantly during summer by way of agricultural practices, $NO_x$ and $SO_2$ emissions are distributed almost uniformly throughout the year (see e.g. BUWAL, 1999).

### 3.2.2. Trace species of mineral dust and sea salt origin

Species of mineral dust- ($Ca^{2+}$, $Mg^{2+}$) and sea salt-origin ($Na^+$, $Cl^-$, and $K^+$) show a completely different seasonal behaviour at the two sites. Although the concentrations of these species exhibit a pronounced seasonal pattern at the southern Alpine site, concentrations are constant throughout the year for the northern Alps (Fig. 3, Table 4). Mineral dust tracers in the southern Alps originate mainly from the Sahara (see Sect. 3.1). The $Ca^{2+}$ concentrations at FG and GG were compared with the number of aerosol filters, recovered at nearby stations, that showed visible Saharan dust

(Fig. 4). For this purpose, the stations at Jungfraujoch (3450 m a.s.l., 6 km from FG) and Plan Rosa (3480 m a.s.l., Italian Alps, 12 km from GG) were used. In agreement with the FG $Ca^{2+}$ concentrations, no seasonal cycle of visible dust on aerosol filters at the Jungfraujoch station (period 1995–1999, C. Zellweger-Fäsi, EMPA, personal communication) was observed. In contrast, Saharan dust observations show a maximum in summer at the Plan Rosa station (time period 1968–1977; Prodi and Fea, 1978) in concert with the seasonal cycle in $Ca^{2+}$ concentrations at GG. Thus, the differences in the seasonality of dust-related species at these two glacier sites is explained by the presence or absence of seasonal contrast in the transport of Saharan dust to the respective sites. Typical pathways for the transport of Saharan dust to Western Europe are shown in Fig. 5 (from Prodi and Fea, 1978), including a direct transport across the Mediterranean Sea (a) and a diverted anticyclonic transport across the Atlantic Ocean (b). Prodi and Fea (1978) showed that the main transport of Saharan dust to the southern Alps occurs during situation (a). The authors related the higher frequency of the dust transport in spring and summer to a more frequent occurrence of the dust-mobilising wind (the "ghibli") in north Africa during the warmer months. From an analysis of the synoptic weather situations for every Saharan dust event observed at Jungfraujoch (period 1995–1999), we deduced that both situations (a and b) contributed almost equally in transporting dust to the northern Alps. However, the question of why this equal representation by both pathways leads to the absence of a seasonal dust cycle in the northern Alps is still open.

The similar annual cycle in sea salt and dust-related species at GG is explained by a coupled transport to the southern Alps during advective south-westerly wind situations (see above). The absence of a seasonal cycle in the concentrations of sea salt species at FG, however, is explained by the transport of sea salt with advective westerly wind situations from the Atlantic Ocean to the northern Alps. These conditions are uniformly distributed throughout the year.

### 3.3. Long-term trends

From the different annual cycles of sea salt and dust related species over the period 1974–1983, it was possible to reconstruct transport paths of these species to the respective Alpine chains. In this section, we investigate whether the obtained information is valid over the entire time period covered by both ice cores. Furthermore, the interpretation of the complete profiles of the anthropogenic species, used in conjunction with existing historical emission data for various countries, could allow for a more precise determination of the source regions for these species.

The comparison of long-term trends in trace species, as archived within the northern vs. southern Alpine chain, was carried out after averaging the ice core data from FG and GG in five-year intervals.

#### 3.3.1. Trace species of anthropogenic origin

Concentration records of $NH_4^+$ and $exSO_4^{2-}$, species with mainly an anthropogenic origin, are shown in Fig. 6. $ExSO_4^{2-}$ represents the portion of $SO_4^{2-}$ which is exclusively formed by the oxidation of $SO_2$ in the atmosphere. The main other sources of $SO_4^{2-}$ in the Alpine region are mineral dust and sea salt (Schwikowski et al., 1999b). In this study, $Na^+$ and $Ca^{2+}$ were used as sea-salt and mineral-dust tracers to quantify the contribution of both sources, respectively. Accordingly, the concentration of $exSO_4^{2-}$ (in $\mu$eq $l^{-1}$) was derived by way of Eq. (1). The ratios, $[SO_4^{2-}]/[Na^+]=0.12$ and $[SO_4^{2-}]/[Ca^{2+}]=0.175$, applied in this calculation were obtained solely from pre-industrial samples.

$$[exSO_4^{2-}]=[SO_4^{2-}]-0.12[Na^+]-0.175[Ca^{2+}]. \quad (1)$$

On average, the contribution of mineral dust-$SO_4^{2-}$ and sea salt-$SO_4^{2-}$ to the overall $SO_4^{2-}$ budget amounts to 12% and 2% for FG, or alternately to 16% and 1% for GG, respectively.

Concentration records of the trace compounds of mainly anthropogenic origin agree well for FG and GG over the 60-year period (Fig. 6, $NO_3^-$ not shown). This result is consistent with results from Preunkert et al. (2000), showing comparable concentration records of $NH_4^+$, $NO_3^-$, and $SO_4^{2-}$ between two Alpine ice cores from Colle Gnifetti (1 km distant from GG) and Col du Dôme (French Alps, 80 km west from GG) for the time period 1982–1991. Thus, species of anthropogenic origin seem to be homogeneously distributed throughout the Alps.

Concentration records of $NH_4^+$ and $exSO_4^{2-}$ reveal a steady increase lasting until the beginning of the 1970s, followed thereafter by a persistent decrease (Fig. 6). In contrast, $NO_3^-$ concentrations increase steadily between 1940 and 1970, but then remain at this high level until 1990. The pre-1970 steep increase in $NO_3^-$ concentrations is due to enhanced NOx emissions from traffic. Although combustion catalysts have been more widely implemented in recent decades, only a weak decline in $NO_3^-$ deposition is observed. Estimates of NOx emissions in Switzerland confirm a steady high level since the 1970s (BUWAL, 1995). To our knowledge, no long-term records from other European countries are available, preventing the determination of the source region for this species. The record of the $NH_4^+$ concentrations mainly reflects $NH_3$ emissions from animal manure and thereby the historical development of livestock. Döscher et al. (1996) compared the $NH_4^+$ record over the period 1780–1980 from Colle Gnifetti (1 km distant from GG) with historical emission estimates, and suggested Europe as the source region of the relatively short-lived precursor species $NH_3$. Due to the lack of emission data for single countries, it was not possible to determine more precisely the source region for $NH_4^+$ from our data sets. The record of $exSO_4^{2-}$, originating from the oxidation of $SO_2$ in the atmosphere, is dominated by anthropogenic $SO_2$ emissions (see also Schwikowski et al., 1999b). The strong increase between 1940 and 1970 is explained by enhanced combustion of fossil fuels. Due to a subsequent enforcement of air pollution-control measures (e.g. desulphurisation of coal, use of low-sulphur fuels, introduction of filters and scrubbers in power plants), $exSO_4^{2-}$ concentrations in the 1990s were again as low as in the 1940s. The evolution of $exSO_4^{2-}$ at both sites

was compared with historical $SO_2$ emission estimates from various European countries (Switzerland, Germany, France, Italy, Austria, Spain) between 1940 and 1990 (Mylona, 1996). Significant correlations were found with $SO_2$ emissions from France and Italy, but not with those from other European countries. This discrepancy is clearly outlined for France, Italy, Switzerland, and Germany (Table 5, all values). The agreement in the trend between the $exSO_4^{2-}$ concentration record at GG and the historical $SO_2$ data for France and Italy is in accordance with the argument of precipitation deriving mainly from the West and Southwest in the southern Alps (see Table 1). In an analogous manner, the major precipitation pattern for the northern Alps (i.e., westerly winds) explains the strong correlation between the $exSO_4^{2-}$ concentration record at FG and specifically the $SO_2$ emission estimates of France.

In addition to the all-inclusive records, the profiles for specifically the summer and winter concentrations of anthropogenic species were generated and are shown in Fig. 7. The samples were classified into summer and winter snow according to the temperature-dependent parameter $\delta^{18}O$. As suggested in Schwikowski et al. (1999a), samples with $\delta^{18}O > -15‰$ and $\delta^{18}O < -19‰$ were related to summer and winter snow, respectively. These limits were based on a comparison of $\delta^{18}O$ values in snow with air temperature. As expected from the seasonal cycle previously determined for 1974-83 (see Sect. 3.2), concentrations of $NH_4^+$ and $exSO_4^{2-}$ in summers are higher than those in the corresponding winters , here illustrated over the entire time period (see Fig. 7). For $NH_4^+$, the trends in summer concentrations agree well between FG and GG. Concentrations of $NH_4^+$ in winter reveal no significant trend at either site, but rather exhibit a nearly constant level of $\sim$3 $\mu$eq/l. $ExSO_4^{2-}$ concentrations, however, show similar trends in winter and summer. In winter, the lifetime of $SO_2$ is significantly longer compared to that of $NH_3$, to the extent that emissions can reach the free troposphere. Furthermore, $NH_3$ emissions peak in summer, whereas $SO_2$ emissions are as high in winter as in summer. In order to investigate source regions at a seasonal resolution, summer and winter concentration records of $exSO_4^{2-}$ were compared again with historical $SO_2$ emission estimations for various European countries (Mylona, 1996).

Similar to the earlier result using the complete $exSO_4^{2-}$ record, significant correlations were only observed with the $SO_2$ emission data from France and Italy (see Table 5). Interestingly, correlation coefficients between the $exSO_4^{2-}$ concentration trends from both ice cores and the French and Italian $SO_2$ emission estimates were much higher in winter compared to summer. This result is an indication that the composition of the free troposphere above the Alpine region, and thus of the advective precipitation at FG and GG in winter, is mainly influenced by $SO_2$ emissions from France and Italy. Due to the shorter residence time of $SO_2$ in the atmosphere in summer, the source region must be much smaller. This geographical limitation is corroborated by the lower correlation coefficients in this season (see Table 5). From the correlations in summer, it can be deduced that the source region of the $exSO_4^{2-}$ observed at FG is primarily France, whereas for GG it includes both France and Italy. Additionally, local sources may influence the composition of the small-scale convective precipitation in summer, leading to the lower correlation coefficients. These results are only partly in agreement with previous findings that concluded the summer $SO_4^{2-}$ record from Col du Dôme (Mont Blanc area, ~80 km to the west) over the last 75 years reflects $SO_2$ emissions from France, Italy, and Spain (Preunkert et al., 2001a). Within the winter season, the same study suggested a larger-scale contamination of the free troposphere with contributions from all of Europe and possibly from the United States.

The estimated summertime source areas for the anthropogenic trace species observed at FG and GG are summarized in Fig. 8a. Because, at either site, no significant correlation was observed between the concentrations of $NH_4^+$, $NO_3^-$, and $exSO_4^{2-}$ (taken as one) and the contributions from mineral dust and sea salt, the deposition of the anthropogenic species in summer occurs independently, in conjunction with convective precipitation as discussed above. In winter, however, concentrations of $NH_4^+$, $NO_3^-$, and $exSO_4^{2-}$ are strongly correlated with those of mineral dust and sea salt tracers at GG. This uniformity indicates that although they have different sources, all ions are deposited together in the southern Alps during advective precipitation from the Southwest (Fig. 8b). At FG, no correlation between the anthropogenic tracers and mineral dust or

sea salt was observed in winter. Thus, the transport of species of anthropogenic origin to the northern Alps in winter is not coupled to that of mineral dust or sea salt. One assumption is that $NH_4^+$, $NO_3^-$, and $exSO_4^{2-}$ are deposited during advective precipitation from the Northwest, this being the second-most frequent precipitation type in the northern Alps in winter (see Table 1, Fig. 8b).

### 3.3.2. Trace species of mineral dust and sea salt origin

Concentration records of $Ca^{2+}$ and $Na^+$ are shown in Fig. 6, representing mineral dust and sea salt tracers. The $Ca^{2+}$ concentrations at both sites reveal strong fluctuations but no consistent trend over the time period investigated. Due to the higher values in summer (see Fig. 7), $Ca^{2+}$ concentrations at GG are generally higher than at FG. As was already observed for the 10-year subset (Fig. 3), $Ca^{2+}$concentrations in summer remain about twice those in winter when considering the entire record. Again, summer and winter concentrations are comparable in the northern Alpine chain and the levels are similar to the winter concentrations at the southern site. It can therefore be assumed that the transport paths of mineral dust to the northern and southern Alps were similar, regardless of the period chosen (see summer and winter situation, Figs. 8a and 8b).

At GG, concentrations of sea salt tracers (e.g. $Na^+$, Fig. 6) reveal no trend, as was the case for the mineral dust tracers. In agreement with the results for the period 1974–1983 (Fig. 3), concentrations in summer are about twice as high as concentrations in winter over the entire time period (Fig. 7). A different behaviour was observed for the sea salt tracers at FG (Fig. 6). These concentrations exhibited a constant value from 1940–1960, increased sharply between 1960 and 1965, and then remained stable at this higher level for the remainder of the time period. The increase at the beginning of the 1960s is observed in both summer and winter concentrations (Fig. 7). This phenomenon was interpreted as a change in the frequency of sea salt- advecting weather conditions (Schwikowski et al., 1999a). This concept is supported by the results of Wanner et al. (1997), which indicated an increasing frequency of zonal weather pat-

terns since the 1960s. These weather situations, mainly accompanied by advective westerly winds, are responsible for the transport of sea salt from the Atlantic to the northern Alps.

Further evidence for a change in the nature of the sea salt transport to the northern Alps at the beginning of the 1960s is demonstrated in Fig. 9. The high correlation between $Ca^{2+}$ and $Na^{+}$concentrations at GG indicates a joint transport of mineral dust and sea salt to the southern Alps during the entire time period 1937–1993. This coupled transport is illustrated schematically in Figs. 8a and 8b, valid for both summer and winter seasons. At FG, $Ca^{2+}$ and $Na^{+}$concentrations are also highly correlated, but only specifically for the period 1945–1961 ($r^2$ = 0.62) (Fig. 9). Hence, during this time period, the main contribution to sea salt deposition in the northern Alps occurred in conjunction with the transport of mineral dust transporting weather situations, as described in Sect. 3.2 (Fig. 5). However, no significant correlation between $Ca^{2+}$ and $Na^{+}$concentrations was observed over the period 1962–1987 ($r^2$=0.04) (Fig. 9), indicating that since 1962, sea salt transport via westerly winds (i.e. directly from the Atlantic Ocean) has predominated (see Figs. 8a and 8b).

## 4. Summary

The Alps represent the largest north-south barrier for air flow in Europe, strongly influencing the weather and hence the distribution of atmospheric trace components. To investigate recent and historical north-south gradients in precipitation chemistry, chemical records from ice cores of two Alpine glaciers (Fiescherhorngletscher (FG): northern Alps, period 1944–1988; Grenzgletscher (GG): southern Alps, period 1937–1994) were compared.

An analysis of “weather types” revealed at both sites a dominance of convective precipitation in the warmer seasons, whereas in the colder seasons advective precipitation from the West into the northern region, and from the Southwest and West into the southern region, is predominant.

The trace species $NH_4^+$, $NO_3^-$, $SO_4^{2-}$, $Ca^{2+}$, $Mg^{2+}$, $Na^+$, $K^+$, and $Cl^-$ were analysed in both ice cores. A comparison of median concentrations did not reveal appreciable differences between the major ions ($NH_4^+$, $NO_3^-$, $SO_4^{2-}$, $Ca^{2+}$, and $Mg^{2+}$), whereas median concentrations of the minor ions ($Na^+$, $K^+$, and $Cl^-$) were twice as high at the northern site. A correlation analysis proved instrumental in assigning the investigated trace species to anthropogenic, sea salt, or Saharan dust origin. Moreover, this analysis indicated that precipitation chemistry in the Alpine region is influenced mainly by trace components of anthropogenic origin. However, at GG, a distinction between sea salt and dust-related species was not forthcoming. The observed high correlation between these species suggested a coupled transport scheme to the southern Alpine region.

A seasonal segregation of the data over the time period 1974–1983, and a comparison of the long-term trends with historical emission data, enabled us to determine source areas and to suggest prevailing transport patterns for both sites:

**A)** The concentrations of the trace species of anthropogenic origin revealed comparable seasonal cycles and historical trends at the northern and southern sites. In summer, anthropogenic species are deposited in a coherent manner during small-scale convective precipitation across the entire Alpine region. Correlation between historical $SO_2$ emissions from various European countries and the ice core-$SO_4^{2-}$ records revealed France (alone), and France and Italy, as source areas for FG and GG, respectively. In winter, advective-precipitation patterns instead lead to the deposition of anthropogenic species. The transport pathways are mainly from the Northwest to the FG site and from the Southwest to the GG site. Both precipitation types exhibit similar compositions, reflecting free-tropospheric conditions in winter, and were shown to represent emissions of France and Italy.

**B)** The concentrations of sea salt- and dust-tracers revealed dissimilar seasonal cycles and historical trends when comparing the northern and southern sites. This is explained by the different transport patterns of these species. The sea salt transport to the southern site is generally coupled to the transport of Saharan dust during precipitation from the Southwest. The Saharan dust input at the northern site occurs during

both west- and southwest-derived precipitation. Before 1960, the deposition of sea salt at the northern site was coupled with dust deposition. However, since the beginning of the 1960s, the predominant sea salt input at this site has occurred via transport from the West, independently from incoming dust. This scenario is consistent with the reported post-1960s increase in the frequency of zonal weather circulation, accompanied by advecting westerly winds into Western Europe.

*Acknowledgements.* We thank T. Blunier, T. Döring, A. Döscher, V. Lavanchy, H. Rufli, and J. Schwander for their participation in the field during the drilling campaign at the Grenzgletscher. The support of the Aargauische Zentralmolkerei, Suhr, and the MIGROS Verteilzentrale Neuendorf for storing the ice cores under stable deep-freeze conditions is gratefully acknowledged. We thank K. Henderson for carefully reading the manuscript and useful comments. This work was partly supported by the Swiss National Science Foundation (Project NFP-31).

## References

Bär, O.: Geographie der Schweiz, Lehrmittelverlag des Kantons Zürich, Schweiz, 247, 1983.

BUWAL: Vom Menschen verursachte Luftschadstoff-Emissionen in der Schweiz von 1900–2010, Schriftenreihe Umweltschutz, 256, Bundesamt für Umwelt, Wald und Landschaft (BUWAL), Bern, Switzerland, 1995.

BUWAL: NABEL-Luftbelastung 1998. Messresultate des nationalen Beobachtungsnetzes für Luftfremdstoffe, Schriftenreihe Umwelt, 311, Bundesamt für Umwelt, Wald und Landschaft (BUWAL), Bern, Switzerland, 1999.

Döscher, A., Gäggeler, H.W., Schotterer, U., and Schwikowski, M.: A 130 years deposition record of sulfate, nitrate and chloride from a high-alpine glacier, Water Air Soil Pollut., 85, 603–609, 1995.

Döscher, A., Gäggeler, H.W., Schotterer, U., and Schwikowski, M.: A historical record of ammonium concentrations from a glacier in the Alps, Geophys. Res. Lett., 23, 2741–2744, 1996.

Eichler, A., Schwikowski, M., Gäggeler, H.W., Furrer, V., Synal, H.-A., Beer, J., Saurer, M., and Funk, M.: Glaciochemical dating of an ice core from the upper Grenzgletscher (4200 m a.s.l.), J. Glaciol., 46, 507–515, 2000a.

Eichler, A., Schwikowski, M., and Gäggeler, H.W.: An Alpine ice core record of anthropogenic HF and HCl emissions, Geophys. Res. Lett., 27, 3225–3228, 2000b.
Eichler, A.: Deposition von Spurenstoffen in Firn und Eis alpiner Gletscher, Untersuchung von Nord-Süd-Gradienten, Ph.D. Thesis, University of Bern, 2000c.
Eichler, A., Schwikowski, M., and Gäggeler, H.W.: Meltwater induced relocation of chemical species in Alpine firn, Tellus 53B, 192–203, 2001.
Finlayson-Pitts, B.J. and Pitts, J.N.: Chemistry of the Upper and Lower Atmosphere, Academic Press, San Diego, etc., 969, 2000.
Fliri, F.: Niederschlag und Lufttemperatur im Alpenraum, Wissenschaftliche Alpenvereinshefte, 24, Innsbruck, Österreich, 112 pp., 1974.
Fliri, F.: Synoptische Klimatographie der Alpen zwischen Mont Blanc und Hohen Tauern, Wissenschaftliche Alpenvereinshefte, 29, Innsbruck, Österreich, 686, 1984.
Gäggeler, H.W., Stauffer, B., Döscher, A., and Blunier, T.: Klimageschichte im Alpenraum aus Analysen von Eisbohrkernen, Schlussbericht NFP 31, Vdf Hochschulverlag AG, ETH Zürich, 1997.
Lavanchy, V.M.H., Gäggeler, H.W., Schotterer, U., Schwikowski, M., and Baltensperger, U.: Historical record of carbonaceous particle concentrations from a European high-alpine glacier (Colle Gnifetti, Switzerland), J. Geophys. Res., 104, 21 227–21 236, 1999.
Legrand, M., Preunkert, S., Wagenbach, D., and Fischer, H.: Seasonally resolved Alpine and Greenland ice core records of anthropogenic HCl emissions over the $20^{th}$ century, J. Geophys. Res., 107, D12, 4139, 10.1029/2001JD001165, 2002.
Lugauer, M., Baltensperger, U., Furger, M., Gäggeler, H.W., Jost, D. T., Schwikowski, M., and Wanner, H.: Aerosol transport to the high Alpine sites Jungfraujoch (3454 m a.s.l.) and Colle Gnifetti (4452 m a.s.l.), Tellus, 50B, 76–92, 1998.
Mylona, S.: Sulphur dioxide emissions in Europe 1880–1991 and their effect on sulphur concentrations and depositions, Tellus, 48 B, 662–689, 1996.
Nickus, U., Kuhn, M., Baltensperger, U., Delmas, R., Gäggeler, H.W., Kasper, A., Kromb-Kolb, H., Maupetit, F., Novo, A., Pichlmayer, F., Preunkert, S., Puxbaum, H., Rossi, G.C., Schöner, W., Schwikowski, M., Seibert, P., Staudinger, M., Trockner, V., Wagenbach, D., and Winiwarter, W.: SNOSP: Ion deposition and concentration in high alpine snow packs, Tellus, 49B, 56–71, 1997.
Nickus, U., Kuhn, M., Novo, A., and Rossi, G.C.: Major element chemistry in Alpine snow along a north-south transect in the eastern Alps, Atmos. Environ., 3, 23, 4053–4060, 1998.

Preunkert, S., Wagenbach, D., Legrand, M., Vincent, C.: Col du Dôme (Mt. Blanc Massif, French Alps) suitability for ice core studies in relation with past atmospheric chemistry over Europe, Tellus, 51B, 993-1012, 2000.

Preunkert, S., Legrand, M., and Wagenbach, D.: Sulfate trends in a Col du Dôme (French Alps) ice core: A record of anthropogenic sulfate levels in the European midtroposphere over the twentieth century, J. Geophys. Res., 106, 31991-32004, 2001a.

Preunkert, S., Legrand, M., and Wagenbach, D.: Causes of enhanced fluoride levels in Alpine ice cores over the last 75 years: Implications for the atmospheric fluoride budget, J. Geophys. Res., 106, 12 619–12 632, 2001b.

Prodi, F. and Fea, G.: Transport and deposition of Saharan dust over Alps, 1. Teil des Tagungsberichtes der 15. Internationalen Tagung für alpine Meteorologie, Grindelwald 19–23 September 1978, Veröffentlichungen der Schweizerischen Meteorologischen Zentralanstalt, 179–182, 1978.

Schotterer, U., Fröhlich, K., Gäggeler, H.W., Sandjordj, S., and Stichler, W.: Isotope records from Mongolian and Alpine ice cores as climate indicators. Climatic Change, 36, 519–530, 1997.

Schwikowski, M., Novo, A., Baltensperger, U., Delmas, R., Gäggeler, H.W., Kasper, A., Kuhn, M., Maupetit, F., Nickus, U., Preunkert, S., Puxbaum, H., Rossi, G.C., Schöner, W., and Wagenbach, D.: Intercomparison of snow sampling and analysis within the alpine-wide snowpack investigation (SNOSP), Water Air Soil Pollut., 93, 67–91, 1997.

Schwikowski, M., Brütsch, S., Gäggeler, H.W., and Schotterer, U.: A high resolution air chemistry record from an Alpine ice core: Fiescherhorn glacier, Swiss Alps, J. Geophys. Res., 104, 13 709–13 720, 1999a.

Schwikowski, M., Döscher, A., Gäggeler, H.W., and Schotterer, U.: Anthropogenic versus natural sources of atmospheric sulphate from an Alpine ice core, Tellus, 51B, 938–951, 1999b.

Schwikowski, M.: Reconstruction of European air pollution from Alpine ice cores, In Cecil, L.D., Thompson, L.G., Steig, E.J., and Green, J.R. eds. Earth Paleoenvironments: Records preserved in Mid and Low Latitude Glaciers, Kluwer Academic/Plenum Publishers, 2003, in press.

Streit, N., Weingartner, E., Zellweger, C., Schwikowski, M., Gäggeler, H.W., and Baltensperger, U.: Characterization of size-fractionated aerosol from the Jungfraujoch (3580 m a.s.l.) using Total Reflection X-Ray Fluorescence (TXRF), Intern. J. Environ. Anal. Chem., 76, 1, 1–16, 2000.

Suter, S., Laternser, M., Haeberli, W., Hoelzle, M., and Frauenfelder, R.: Cold firn and ice of high-altitude glaciers in the Alps: Measurements and distribution modelling, J. Glaciol., 47, 85–96, 2001.

Van der Knaap, W. O., van Leeuwen, J. F. N., and Ammann, B.: Seven years of annual pollen influx at the forest limit in the Swiss Alps studied by pollen traps: relations to vegetation and climate, Rev. Palaebot. Palynol., 117, 31–52, 2001.

Van de Velde, K., Ferrari, C., Barbante, C., Moret, I., Bellomi, T., Hong, S., and, Boutron, C.: A 200 year record of atmospheric cobalt, chromium, molybdenum, and antimony in high altitude Alpine firn and ice, Environ. Sci. Technol., 33, 3495–3501, 1999.

Van de Velde, K., Barbante, C., Cozzi, G., Moret, I., Bellomi, T., Ferrari, C., and Boutron, C.: Changes in the occurrence of silver, gold, platinum, palladium, and rhodium in Mont Blanc ice and snow since the 18th century, Atmos. Environ., 34, 3117–3127, 2000.

Wagenbach, D. and Geis, K.: The mineral dust record in a high altitude Alpine glacier (Colle Gnifetti, Swiss Alps), In Leinen, M. and Sarnthein, M. eds. Paleoclimatology and Paleometeorology: Modern and Past Patterns of Global Atmospheric Transport, Kluwer Academic Publishers, Dortrecht, 543–564, 1989.

Wagenbach, D., Münnich, K.O., Schotterer, U., and Oeschger, H.: The anthropogenic impact on snow chemistry at Colle Gnifetti, Swiss Alps, Ann. Glaciol., 10, 183–187, 1988.

Wanner, H., Rickli, R., Salvisberg, E., Schmutz, C., and Schüepp, M.: Global climate change and variability and its influence on Alpine climate – concepts and observations, Theor. Appl. Climatol., 58, 221–243, 1997.

Weiss, D., Shotyk, W., Appleby, P. G., Kramers, J. D., and Cheburkin, A. K.: Atmospheric Pb deposition since the Industrial Revolution recorded by five Swiss peat profiles: Enrichment factors, fluxes, isotopic composition, and sources, Environ. Sci. Techn., 33, 1340–1352, 1999.

**Table 1.** "Weather types" leading to the most frequent precipitation in the northern and southern Alps in the vicinity of FG and GG, respectively, and for the given seasons (after Fliri, 1984). The weather types as indicated in bold letters are responsible for the largest fraction of precipitation within the respective season. See text for descriptions of the weather types identified.

| | FG (north) | | GG (south) | |
|---|---|---|---|---|
| | convective | advective | convective | advective |
| Spring | L | **W** | L | **SW** |
| Summer | **L** | W | **L** | W |
| Autumn | L | **W** | L | **SW** |
| Winter | | **W**, NW | | **W**, SW |

**Table 2.** Median concentrations of the trace ions in the FG and GG ice cores, and for each ion, the ratios between the two sites (FG/GG) (time period 1945–1983).

| Cation | c ($\mu$eq l$^{-1}$) | | | Anion | c ($\mu$eq l$^{-1}$) | | |
|---|---|---|---|---|---|---|---|
| | FG | GG | **FG/GG** | | FG | GG | **FG/GG** |
| $NH_4^+$ | 4.37 | 4.96 | **0.88** | $SO_4^{2-}$ | 7.63 | 8.0 | **0.95** |
| $Ca^{2+}$ | 5.0 | 4.60 | **1.09** | $NO_3^-$ | 2.69 | 2.43 | **1.10** |
| $Mg^{2+}$ | 0.75 | 0.83 | **0.90** | | | | |
| $Na^+$ | 1.22 | 0.57 | **2.14** | $Cl^-$ | 1.46 | 0.72 | **2.03** |
| $K^+$ | 0.54 | 0.27 | **2.0** | | | | |

**Table 3.** Sources of trace species deduced from the correlation analysis (significant at the 0.01 level).

| FG | | GG | |
|---|---|---|---|
| Anthropogenic | $NH_4^+$, $NO_3^-$, $SO_4^{2-}$ | Anthropogenic | $NH_4^+$, $NO_3^-$, $SO_4^{2-}$, $K^+$ |
| Dust | $Ca^{2+}$, $Mg^{2+}$ | Dust/Sea salt | $Ca^{2+}$, $Mg^{2+}$, $Na^+$, $Cl^-$, $K^+$ |
| Sea salt | $Na^+$, $Cl^-$, $K^+$ | | |

**Table 4.** Summer/Winter (Su/Wi) – concentration ratios of the trace species of **(a)** mainly anthropogenic origin, and **(b)** natural origin, for FG and GG (time period 1974–1983).

**(a)**

| Su/Wi | $NH_4^+$ | $NO_3^-$ | $SO_4^{2-}$ |
|---|---|---|---|
| FG | 3.0 | 1.7 | 1.9 |
| GG | 3.0 | 1.6 | 2.3 |

**(b)**

| Su/Wi | $Ca^{2+}$ | $Mg^{2+}$ | $Na^+$ | $Cl^-$ | $K^+$ |
|---|---|---|---|---|---|
| FG | 0.9 | 1.1 | 1.0 | 1.3 | 1.1 |
| GG | 1.7 | 2.3 | 1.9 | 2.0 | 1.8 |

**Table 5.** Correlations between historical $SO_2$ emission estimates from France, Italy, Switzerland, and Germany (Mylona, 1996) and $exSO_4^{2-}$ deposition at FG and GG (5-year averages, All: entire data set, Su: summer values, Wi: winter values). Significant correlations are given in bold (0.01 level).

| $r^2$ | France | Italy | Switzerland | Germany |
|---|---|---|---|---|
| GG | **All 0.77** | **All 0.69** | All 0.40 | All 0.35 |
| | **Su 0.71** | **Su 0.59** | Su 0.40 | Su 0.36 |
| | **Wi 0.87** | **Wi 0.80** | Wi 0.34 | Wi 0.48 |
| FG | **All 0.64** | All 0.46 | All 0.26 | All 0.22 |
| | **Su 0.55** | **Su 0.37** | Su 0.15 | Su 0.15 |
| | **Wi 0.87** | **Wi 0.76** | Wi 0.21 | Wi 0.43 |

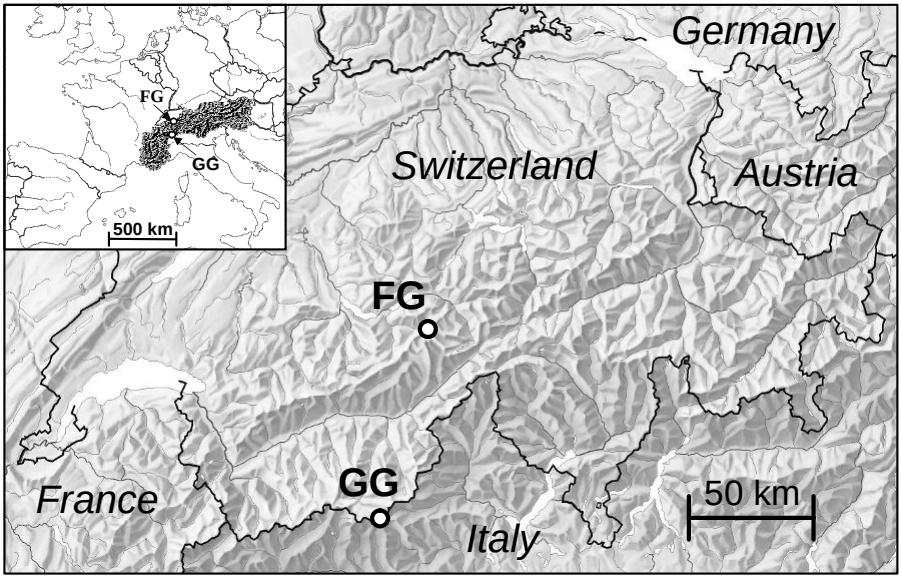


**Fig. 1.** Topographic map of Switzerland and the bordering countries, indicating the locations of the drilling sites at FG and GG. Inset provides a wider view of Western Europe, with again the Alps and both drilling sites indicated.



ACPD
4, 71–108, 2004

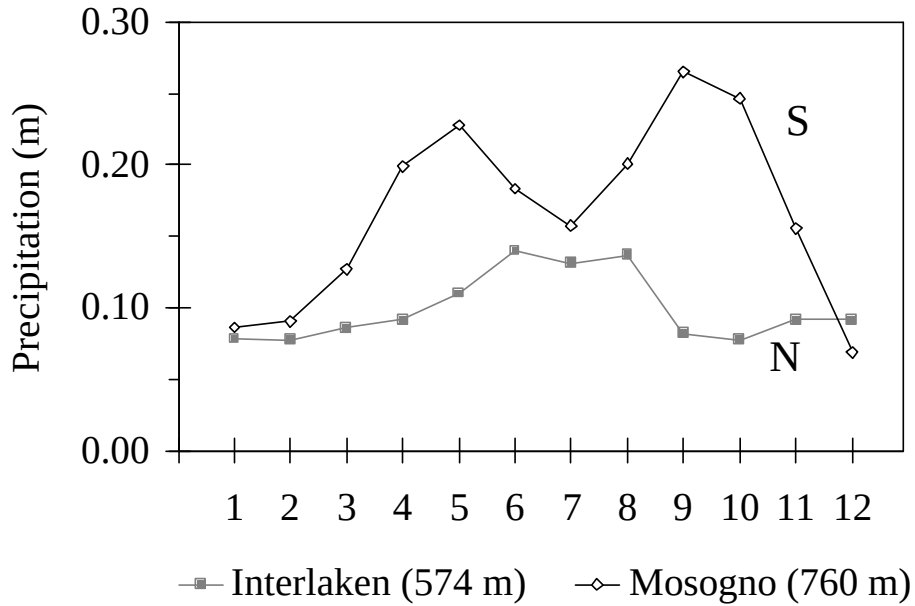


**Fig. 2.** Monthly amounts of precipitation at the weather stations Interlaken and Mosogno (averaged over the period 1961–1994), representing situations typical of the northern (N) and southern Alps (S), respectively.

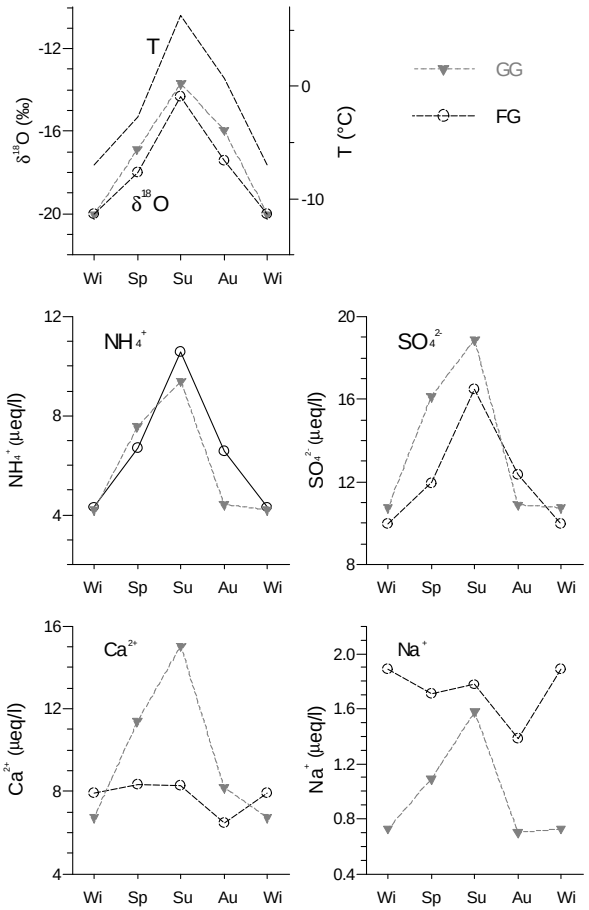


**Fig. 3.** Annual cycle within $\delta^{18}O$ values, $NH_4^+$, $SO_4^{2-}$, $Ca^{2+}$ , and $Na^+$ concentrations for FG (circles) and GG (triangles) over the period 1974–1983. $\delta^{18}O$ values are shown in comparison to air temperatures at Col du Gd. St. Bernard (2480 m a.s.l.).

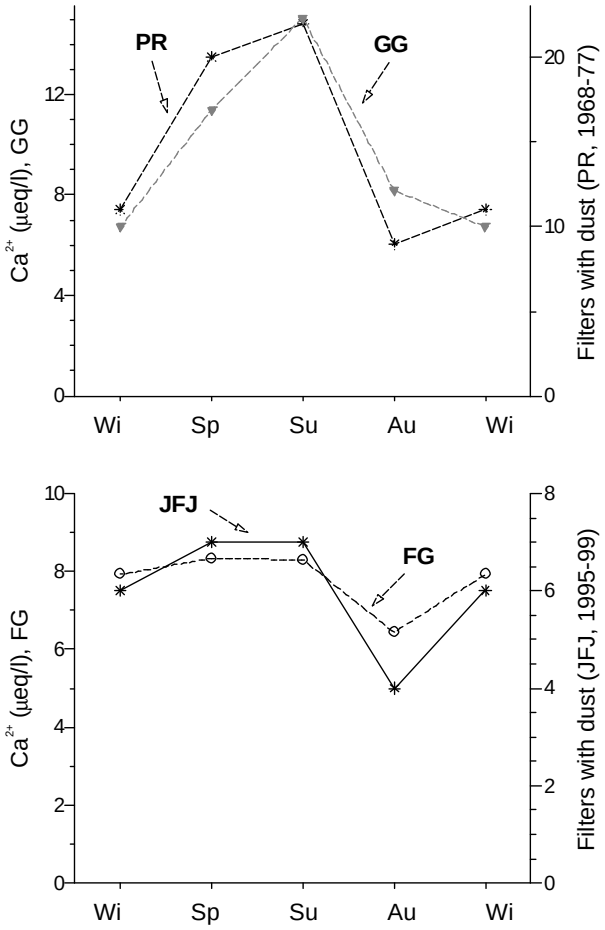


**Fig. 4.** Annual cycle of $Ca^{2+}$ concentrations (dashed lines) at GG (top) and FG (bottom) along with the number of filters with Saharan dust (lines) observed at nearby stations Plan Rosa (PR, 1968–1977) and Jungfraujoch (JFJ, 1995–1999).

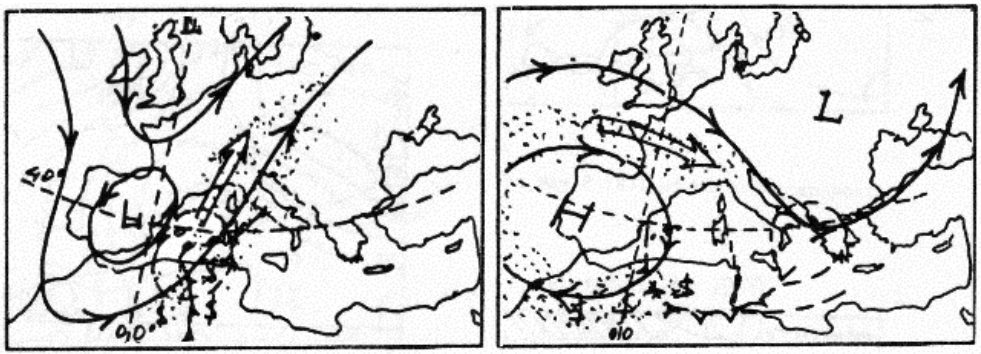


**Fig. 5.** Flow patterns at the 500 mbar level, favourable for direct transport (left), and diverted anticyclonic transport (right), of Saharan dust (reproduced from Prodi and Fea, 1978, with permission from MeteoSchweiz).



ACPD
4, 71–108, 2004

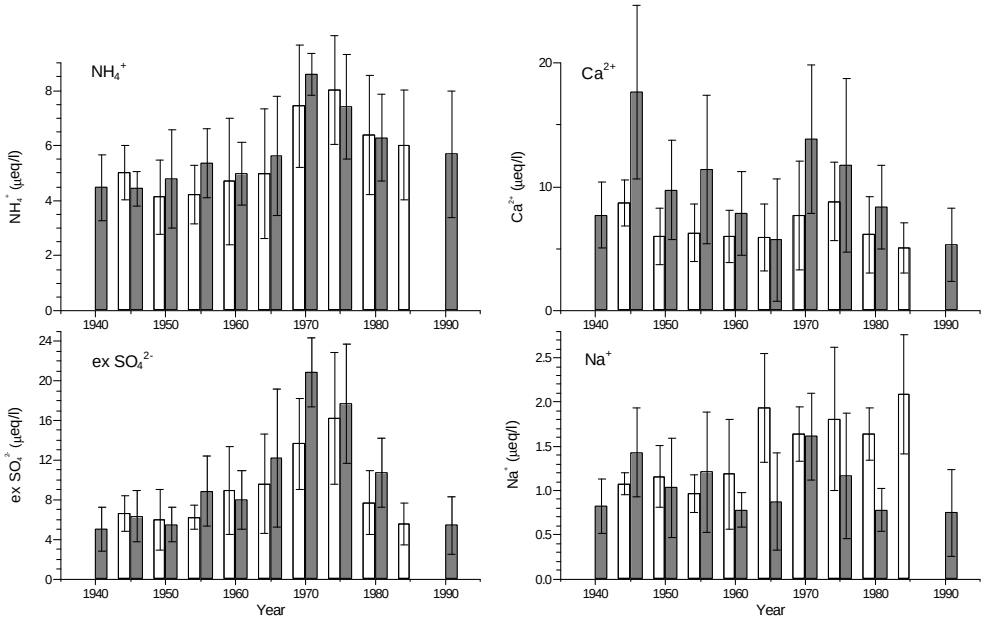


**Fig. 6.** Temporal records of the $NH_4^+$, $exSO_4^{2-}$, $Ca^{2+}$, and $Na^+$ concentrations (5-year means) for FG (white bars) and GG (grey bars).

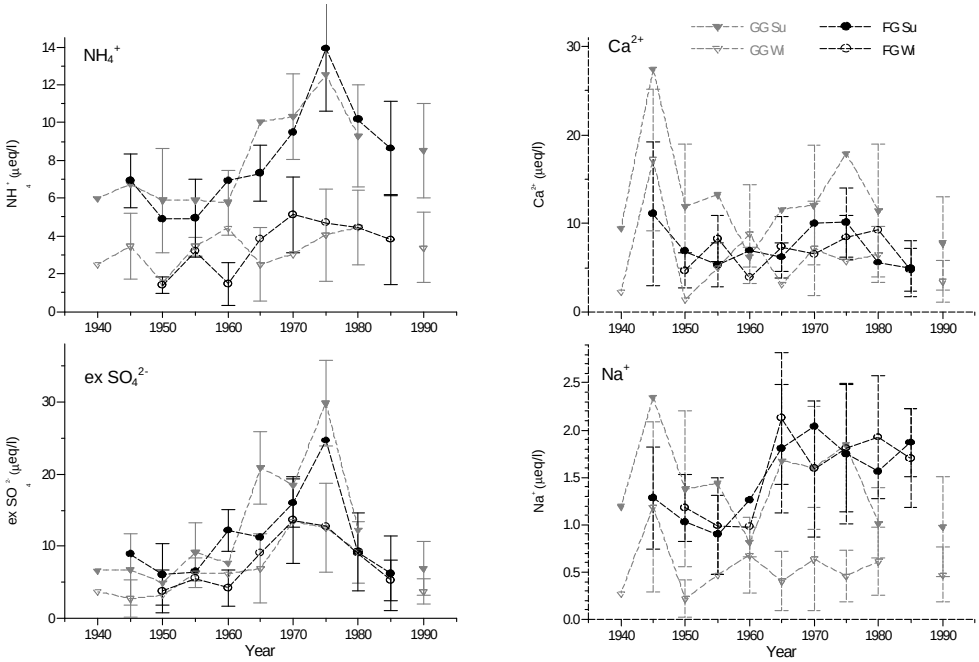


**Fig. 7.** Temporal records of the $NH^{4+}$, $exSO_4^{2-}$, $Ca^{2+}$, and $Na^+$ concentrations (5-year means) for FG (white bars) and GG (grey bars).

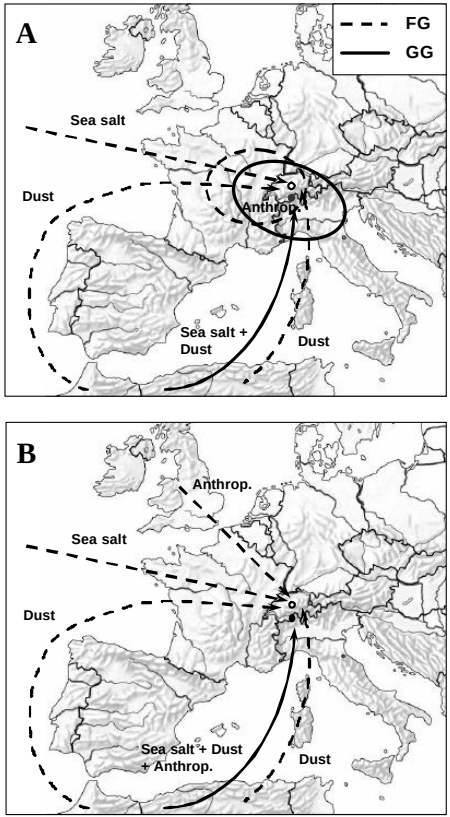


**Fig. 8.** Conceptual model of transport pathways and source areas for sea salt, dust, and species of anthropogenic origin observed at FG (dashed lines) and GG (solid lines) in summer **(a)** and winter **(b)**. The transport path of sea salt to the FG site is valid since the beginning of the 1960s. Previously, the major portion of sea salt was transported in conjunction with Saharan dust.

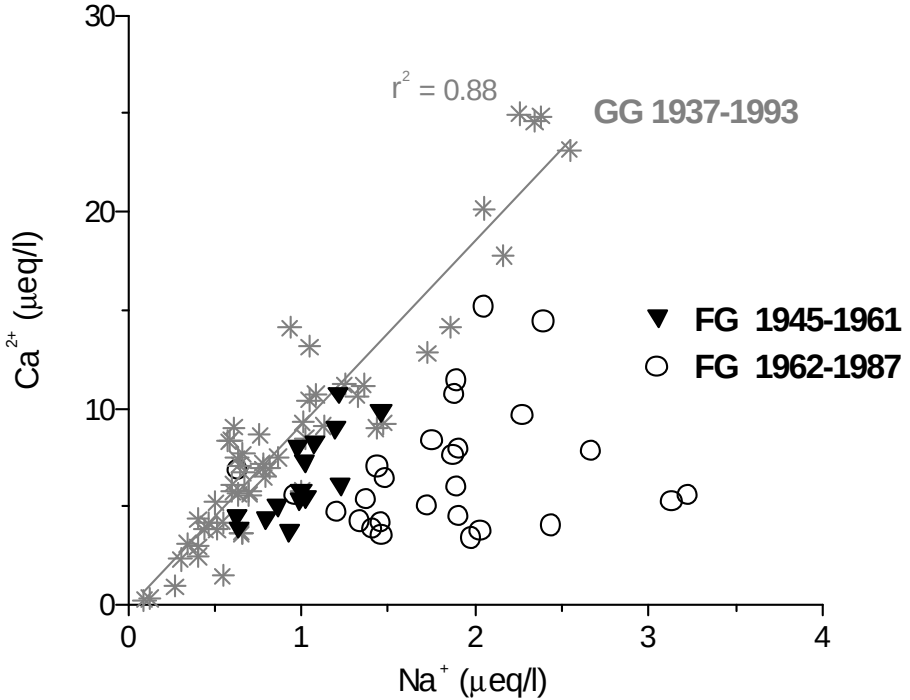


**Fig. 9.** Correlation between annual means of $Ca^{2+}$ and $Na^+$ concentrations for GG over the period 1937–1993 (grey stars, regression line) and FG (1945–1961: inverted triangles, 1962–1987: circles).



ACPD
4, 71–108, 2004